Activated biocarbons obtained from lignocellulosic precursors as potential adsorbents of ammonia

Katarzyna Jedynak [1], Barbara Charmas [2]

[1] Jan Kochanowski University, Faculty of Exact and Natural Sciences, Institute of Chemistry, Uniwersytecka Str. 7, 25-406 Kielce, Poland

[2] Maria Curie-Sklodowska University, Faculty of Chemistry, Institute of Chemical Sciences, Maria Curie-Sklodowska Sq. 3, 20-031 Lublin, Poland

Corresponding author: kjedynak@ujk.edu.pl (Katarzyna Jedynak)

Abstract: The investigated materials were new biocarbons: FC (Fir Cone), FS (Fir Sawdust), FB (Fir Bark), BS (Birch Sawdust), BB (Birch Bark), AS (Acacia Sawdust), AB (Acacia Bark), OS (Oak Sawdust), OB (Oak Bark), HS (Hornbeam Sawdust)) obtained via pyrolysis and CO_2 activation of wood waste (lignocellulosic biomass). In order to study the influence of the carbon precursor on the physicochemical properties of biocarbons there were used the precursors: cones, sawdust, and bark of various tree species. The obtained adsorbents were characterized based on the results, of the N_2 adsorption, scanning electron microscopy (SEM), elemental analysis (CHNS), thermogravimetry (TG), derivative thermogravimetry (DTG), and differential thermal analysis (DTA), Fourier Transform Infrared Spectroscopy FT-IR (ATR) and the Boehm's titration method as well as pH_{pzc} (the point of zero charge). The adsorption capacity and the temperature-programmed desorption (TPD) of ammonia were also studied. The obtained activated biocarbons were characterized by the large specific surface area (515 to 1286 m^2/g) and the total pore volume (0.27 to 0.46 cm^3/g) as well as the well-developed microporous structure (76 - 90%). The maximum NH_3 adsorption capacity of the activated biocarbon was determined to be 2.93 mmol/g (FC (Fir Cone)). These results prove that the lignocellulosic precursors are appropriate for preparation of environmentally friendly and cost-effective biocarbons.

Keywords: activated biocarbons, various carbon precursors, physical activation, physicochemical properties, ammonia adsorption

1. Introduction

Environmental pollution caused by the dynamic development of the industrial sector is a serious problem. Every day, huge amounts of toxic gases and industrial waste are released into the environment (Bazan-Wozniak et al., 2017). This type of pollution poses a threat to humans and animals. Air pollution resulting from excessive greenhouse gas emissions into the atmosphere is a global problem (Basharnavaz et al., 2020). Extremely dangerous environmental pollutants, originating from car exhaust emissions, oil refineries or coal gasification and others, include gases such as: SO_2, CO, NO, NO_2, H_2S, HCN, NH_3. Detecting these toxic gases is a major technological challenge as they are harmful even at low concentrations and can lead to death at high concentrations (Basharnavaz et al., 2020; Huang et al., 2008). Therefore, it is important to look for good, cheap and unconventional adsorbents that can contribute to the environmental sustainability and offer commercial benefits purposes in the future. Such materials can be biocarbons, the main products of biomass pyrolysis. They are competitive with other carbon materials (nanotubes, graphene, activated carbon) as they can be produced from virtually all biomasses (Břendová et al. 2017; Cho et al., 2019; Jedynak and Charmas, 2021). An additional advantage is the ease of activation and modification, which allows for significant development of their porous structure and surface functionalization (Wiśniewska et al., 2022). The surface reactivity and adsorption properties of the finally obtained carbon materials are

significantly influenced by the presence of surface functional groups. The final properties and surface functionalities of the obtained biocarbons are decisively affected by the nature of the charred precursors as well as the conditions of the pyrolysis and activation process (Contescu et al., 2018). Different types of carbon precursors are used in the production of biocarbons. Due to its common availability, low price and efficiency, the lignocellulosic biomass is a promising raw material (Nor et al., 2013; Contescu et al., 2018). The biomass rich in lignocellulose is hardly decomposable waste from various industries (paper, agri-food, wood). The development of lignocellulosic biomass technologies focuses mainly on biorefining, the products of which are: biomaterials, biofuels and biochemicals (Lalak et al., 2014; Ballet, 2011). The lignocellulosic biomass is composed of a cell wall including cellulose (40 - 55%), hemicellulose (24 - 40%), lignin (18 - 25%) and inorganic extracts as well as compounds occurring in the minority, i.e. ash (Robak and Balcerek, 2017; Lalak et al., 2014). The share of individual biomass fractions depends on its type. The amount of each component is variable and depends on many factors such as: part of the plant, species, age of the plant, etc. (Bogumił, 2016). A number of different lignocellulosic precursors have been used to produce biocarbons: rice husk, cotton stalks (Saletnik et al., 2017; Nor et al., 2013), sawdust (Ma et al., 2020; Borhan et al., 2014), cones (Nowicki et al., 2013), cereal straw (Břendová et al. 2017), corn cobs, fruit stones (Zięzio et al. 2020), sunflower husks, nut shells (Wiśniewska et al., 2022) and many others.

The range of biochars application is numerous. For example, they can replace more expensive or less effective adsorbents that are currently used in waste gas treatment processes, e.g.: SO_2 [Saad et al., 2020; Samojeden and Grzybek, 2017], NO [Samojeden and Grzybek, 2016], etc. The possibility of additional surface modification of biocarbons has a positive effect on the specific surface area and porosity development, causing an increase in the adsorption efficiency of these materials [Samojeden and Grzybek, 2016].

Besides nitrous oxide (N_2O), ammonia is one of the most common compounds in the atmosphere (Huang et al., 2008; Rodrigues et al., 2007). This poisonous gas is a valuable chemical raw material used in industry (Yeom and Kim, 2017). When the ammonia content in the atmosphere exceeds 35 ppm, it has a negative impact on human and animal health (Chen et al., 2016). Therefore, it is very important to eliminate it from the surrounding atmosphere for the sake of the safety of the natural environment and living organisms. Effective adsorbents with great adsorption capacity can be an alternative in capturing toxic gases (ammonia and others). Such effective adsorbents can be biocarbons with specially designed properties.

To sum up, the prospective research on the preparation of biocarbons for the adsorption of gaseous pollutants from the air should focus on optimizing adsorption properties, using modern production technologies, studying the impact of environmental factors and developing effective recovery and regeneration methods. Such research is crucial for further development and improvement of the air quality, which will benefit us all. Therefore the aim of the research was to obtain activated biocarbons from different lignocellulosic precursors (cone, sawdust, bark) as well as investigation of the impact of a carbon precursor type on the physicochemical properties and sorption capacity as regards the gas phase impurities, specifically ammonia.

2.   Materials and methods

2.1. Biocarbons preparation

The precursors of active biocarbon were cones, sawdust and bark of various tree species. The biomass (bark, cones) was collected from forest areas, while the sawdust was obtained from the sawmill. In order to get rid of impurities, the precursors were washed with running water, then the distilled water and dried for 24 h at 105 ºC in the laboratory oven. Then the biomass was ground in a grinder (MF 10, IKA, Germany) - a grain size fraction of less than 1 mm. The biomass prepared in this way was subjected to the pyrolysis process (tube furnace: MRT-4, Czylok, Poland). The three-stage pyrolysis in N_2 atmosphere (20 dm³/h) was performed: I stage: 20 – 180 °C (2 °C/min, 2h); Stage II: 180 – 400 °C (2 °C/min, 2h); Stage III: 400 – 800 °C (2 °C/min, 2h). Biocarbons were activated to develop a porous structure. Activation was performed in the following manner: from 20 °C to 800 °C (heating 10 °C/min, N_2 atmosphere, 20 dm³/h), then the gas was switched into CO_2 (10dm³/h) and the biocarbon was activated at 800 °C for 7 h. The samples were cooled in the N_2 atmosphere to room

temperature. The obtained biocarbons were designated FC (Fir Cone), FS (Fir Sawdust), FB (Fir Bark), BS (Birch Sawdust), BB (Birch Bark), AS (Acacia Sawdust), AB (Acacia Bark), OS (Oak Sawdust), OB (Oak Bark), HS (Hornbeam Sawdust).

2.2. Characterization of the obtained biocarbons

The low-temperature nitrogen adsorption/desorption isotherms were measured at 77 K using the ASAP 2020 volumetric analyzer (Micromeritics Inc., Norcross, GA, USA) in the Structural Research Laboratory at Jan Kochanowski University in Kielce. Just before the measurements, all samples were degassed at 200 °C for at least 2 hours.

The biocarbons morphology was studied by means of SEM DualBeam Quanta 3D FEG FEI. The voltage of 5kV was applied in the measurements.

The elemental analysis (CHNS) was performed using the Elementar Vario Micro Cube analyzer (Elementar, Langenselbold, Germany). All samples were dried to constant weight before the measurements.

The thermal stability as well as the volatile and fixed carbon content in the biocarbons were determined using a Derivatograph C (Paulik, Paulik & Erdey, MOM, Budapest). The tested materials (about 10 mg) were placed in the corundum crucible. Al_2O_3 was used as the reference sample. The analysis was performed in air and nitrogen atmospheres in the temperature range from 20 to 1200 °C (heating rate 10 °C/min). The TG, DTG and DTA curves were registered. The volatile carbon content (%VC, ash-free) was determined from the TGA data in the N_2 atmosphere in the temperature range of 200 – 900 °C (TG_{900-N2}) assuming that moisture desorption occurs up to 200 °C. The moisture content (%H) was determined as the loss of mass at 200 °C in the nitrogen atmosphere. The ash content (%A) was determined as the residue after the total thermal degradation of the material in the O_2 atmosphere at 1200°C ($TG\%_{1200-O2}$). The fixed carbon (%TSC, ash-free) was given as the difference between $TG\%_{1200-O2}$ and $TG\%_{900-N2}$. %VC, %A and %TSC were expressed in relation to the dry weight. The proportion of the biocarbons thermostable fraction (%C_{thermo}, resistant to the thermal degradation, ash-free) as the content of stable substances (%TSC) in relation to the sum of the volatile (%VC) and fixed (%TSC) substances (Calvelo Pereira et al., 2011) was also determined. This is a parameter used to assess the level of organic matter stability in organic materials (Cárdenas-Aguiar et al., 2019).

The Perkin-Elmer Spectrum 400 FT-IR/FT-NIR spectrometer (Perkin-Elmer, Waltham, MA, USA) with the smart endurance single bounce diamond, attenuated total reflection (ATR) cell was used for the infrared spectra recording. The 4000 – 650 cm⁻¹ range spectra were obtained from the coaddition of 40 scans with the 4 cm⁻¹ resolution. All samples were dried and powdered in the agate mortar before being measured.

The Boehm's titration method (Boehm, 2002) was used for determination of the functional acidic and basic oxygen surface groups. The 0.2 g mass weights of the biocarbons were dispersed in the sodium bicarbonate, sodium carbonate, sodium hydroxide and sodium ethoxide solutions (V = 25 cm³, all at the concentration of 0.1 mol/dm³) for determination of the functional acidic groups. However, hydrochloric acid (0.05 mol/dm³) was used for the determination of the total basic groups. After shaking for 48 h at room temperature the suspensions were filtrated and 10 cm³ of the filtrate was titrated with 0.1 mol/dm³ HCl for determination of the acidic groups and with 0.05 mol/dm³ NaOH for the total basic group determination. The titration endpoint was determined using the methyl orange indicator.

The carbon pH_{pzc} (point of zero charge) was analyzed by means of the method used in (Rivera-Utrilla et al., 2001; Lim et al. 2013). At first, the 0.01 mol dm⁻³ NaCl solution was prepared. Then the pH was brought to that between 3 and 12 adding 0.1 or 1 mol dm⁻³ HCl and 0.1 or 1 mol dm⁻³ NaOH. The carbon materials samples were added to the solutions with a suitable pH value. Next, they were shaken in the incubator (Orbital Shaker—Incubator ES-20, Grant-bio) for 240 min at 298 K. Next the final pH value was measured. There were determined the relationships between the final and initial values of pH. The pH_{pzc} indicates the intersection point of the experimental curves and $pH_{initial} = pH_{final}$ line (Rivera-Utrilla et al. 2001; Lim et al. 2013). A pH-meter (inoLab pH 730, WTW) was used for measuring the pH value.

The pulse chemisorption and temperature-programmed desorption (TPD) measurements of ammonia were made using the automatic AutoChem II 2920 analyzer (Micromeritics, Norcross, GA, USA). Before testing all biocarbons were degassed at 200 °C for 2 h (ASAP 2020, Micromeritics, Norcross, GA, USA). The first stage of the measurements was the stabilization of the material (50 mg of biocarbon in the quartz reactor) in the helium atmosphere at the temperature of 250 °C (20 °C/min) for 40 min.

The chemisorption studies were carried out at the two temperatures: 0 °C and 20 °C. The standard gas (10% NH_3 in helium) was dosed from the loop of defined volume. The TCD detector registered the next doses. Dosing was performed until the surface of the analyzed material was saturated. The total amount of gaseous ammonia adsorbed on the biocarbon surface was calculated. In the next stage the experiments of thermo-programmed desorption were performed. The temperature increased from the measurement temperature, at which the chemisorption process was initially conducted to 250 °C (with the temperature increase rate of 10 °C/min).

2.3. Calculations

The porous structure standard parameters: specific surface area, pore volume as well as pore size distribution were determined based on the experimental nitrogen adsorption isotherms. Determination of the specific surface area (S_{BET}) was made in the range of the relative pressure from 0.05 to 0.20 taking into account the nitrogen molecule surface area equal to 0.162 nm^2 (Brunauer et al., 1938). Determination of the total pore volume (V_t) was made from one point of the adsorption isotherm at the relative pressure $p/p_0 = 0.99$ (Kruk and Jaroniec, 2001). To calculate the pore size distribution functions (PSDs), the non-local density functional (NLDFT) method was applied for the carbon slit-shaped pores which characterizes the surface energetical heterogeneity and geometrical corrugation (Jagiello and Olivier, 2013; Jagiello and Olivier, 2013a). The calculations were made applying the numerical program SAIEUS (Micromeritics). The maxima of the PSD curves were used to determine the micropore widths, w_{mi}. Microporosity, expressed in % was calculated as the ratio of the micropore volume V_{mi} to the total pore volume V_t.

The concentration of individual functional groups determined by the Boehm method was calculated from the equation (Eq. 1):

$$C = ((V_1-V_2)*C_t*DF)/m \tag{1}$$

where: C - concentration of specific surface groups [mmol/g], V_1 – titrant volume used for titration of the blank solution [dm^3], V_2 – titrant volume used for titration of the filtrate solution [dm^3], C_t – concentration of the titrant solution [mol/dm^3], DF – dilution factor, m – sample mass [g].

3. Results and discussion

3.1. Porous structure parameters

Fig. 1a,b presents the experimental isotherms of adsorption-desorption of nitrogen as well as pore volume distribution functions. The analyzed isotherms are type I according to the IUPAC classification. All obtained adsorbents are characterized by largely developed microporosity, as evidenced by the high adsorption values at low relative pressures. The very small share of mesopores confirms the almost parallel course of isotherms to the relative pressure axis in the medium and high pressure ranges. The pore volume distribution functions (Fig. 1c,d) contain one maximum indicating the presence of micropores in the biocarbons under study. The structural parameters characterizing the porosity of the studied biocarbons, determined based on the experimental nitrogen adsorption isotherms (Fig. 1a,b) are presented in Table 1. The obtained results show that activation with CO_2 leads to effective development of the surface and porous structure of the tested materials. The biocarbon obtained from cones (FC) is characterized by a strongly developed porous structure, which can be correlated with a large specific surface area (1286 m^2/g) and pore volume (0.67 cm^3/g) with a significant proportion of micropores (78%). The biocarbons obtained from sawdust (S_{BET} 609 - 898 m^2/g) are characterized by less developed porosity and those obtained from bark (S_{BET} 515 - 783 m^2/g) are characterized by the least developed porosity. The penultimate column shows the dimension of

the micropores determined with the maximum distribution function (0.57 - 0.70 nm). All tested biocarbons are characterized by a developed microporous structure (76 - 90%).
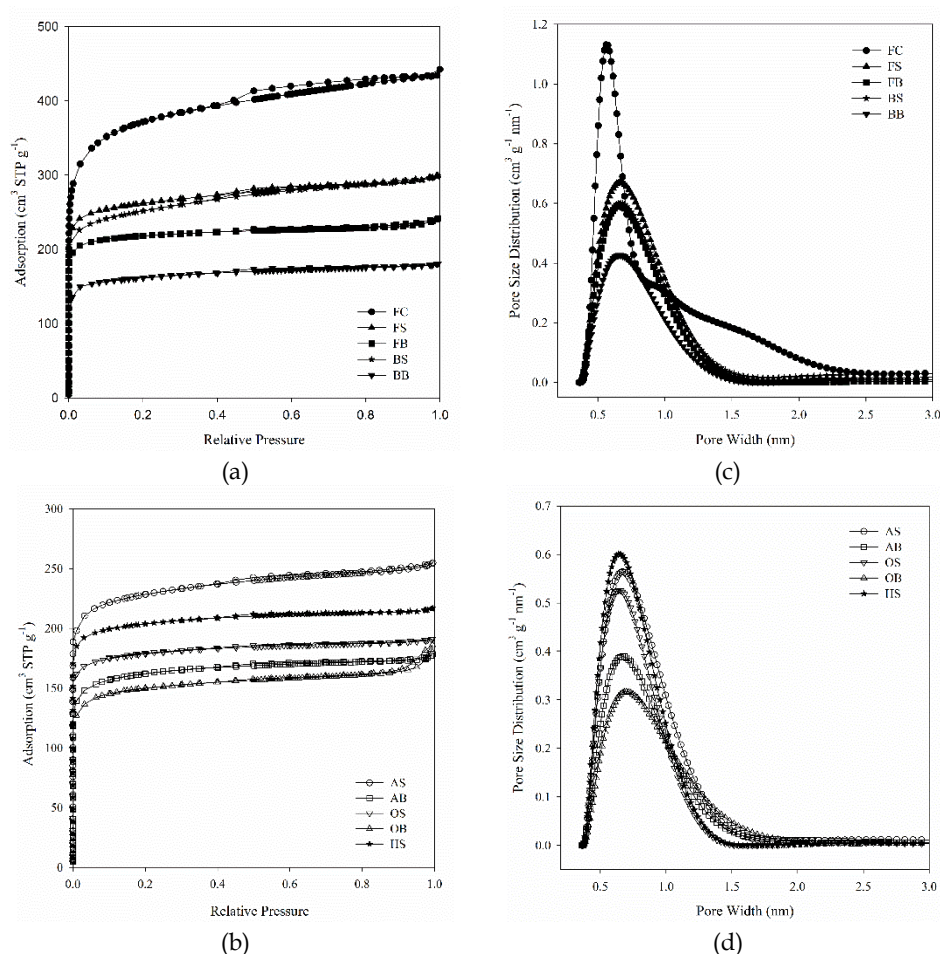

Fig. 1. Nitrogen adsorption-desorption isotherms (a,b) and pore size distribution (c,d) for the studied biocarbons (FC (Fir Cone), FS (Fir Sawdust), FB (Fir Bark), BS (Birch Sawdust), BB (Birch Bark), AS (Acacia Sawdust), AB (Acacia Bark), OS (Oak Sawdust), OB (Oak Bark), HS (Hornbeam Sawdust))

Table 1. Structural parameters of the biocarbons

Biocarbons	S_{BET} (m²/g)	V_t (cm³/g)	$V_{ultraDFT}$ (cm³/g)	$V_{microDFT}$ (cm³/g)	w_{miDFT} (nm)	Microporosity (%)
FC	1286	0.67	0.22	0.52	0.57	78
FS	898	0.46	0.15	0.38	0.67	83
FB	746	0.37	0.13	0.32	0.65	87
BS	866	0.46	0.13	0.35	0.67	76
BB	553	0.28	0.09	0.23	0.65	82
AS	783	0.39	0.12	0.33	0.67	85
AB	555	0.27	0.08	0.24	0.68	89
OS	609	0.30	0.12	0.27	0.64	90
OB	515	0.28	0.07	0.22	0.70	79
HS	695	0.34	0.14	0.30	0.64	88

S_{BET} - the BET specific surface area; V_t - the pore volume; $V_{ultraDFT}$ - the ultramicropores volume (pores width < 0.7 nm) obtained by the DFT method; $V_{microDFT}$ - the micropores volume (pores width < 2 nm) obtained by the DFT method; obtained from the difference of V_t and V_{mi}; w_{miDFT} - micropore diameter at the maximum of the PSD curve obtained by the DFT method; Microporosity - the micropores share.

In order to visualize the topography of the surface and porous structure of the obtained biocarbons, scanning electron microscopy (SEM) was used. The diverse morphology of the obtained activated biocarbons is significantly influenced by the structure and composition of the initial precursor: wood species, waste structure (bark, sawdust), hardness because these features determine the formation of the so-called primary porosity, which develops differently, creating porosity of carbon materials in the processes of pyrolysis and activation. The conditions of pyrolysis and activation in the presented studies were the same, therefore the diversity of the structure and porosity of the obtained biocarbons results from the different structure of the starting waste materials. The SEM images for the biocarbon obtained from fir cones (Fig. 2a) confirm a strongly developed porous structure. We observe pores of different sizes and shapes. This variation, which was mentioned earlier, is clearly visible when comparing the structure of biocarbons obtained from sawdust, e.g. fir, birch and hornbeam (Fig. 2b-d). As can be seen, biocarbons obtained from the sawdust maintained the channel structure of the precursor partially (Yang et al., 2017; Borhan et al., 2014). When the individual SEM images are analyzed, there can be seen differences in the structure of biocarbons resulting from different structures of different trees. Oak and acacia biocarbons are characterized by a different structure (Fig. 2e,f). The structure of the bark is different from that of sawdust, it is rougher which affects the structure of the resulting biocarbons. In this case, the differences in the structure of biocarbons obtained from sawdust (Fig. 2b-f)) and bark (Fig. 2g-j) are clearly visible.
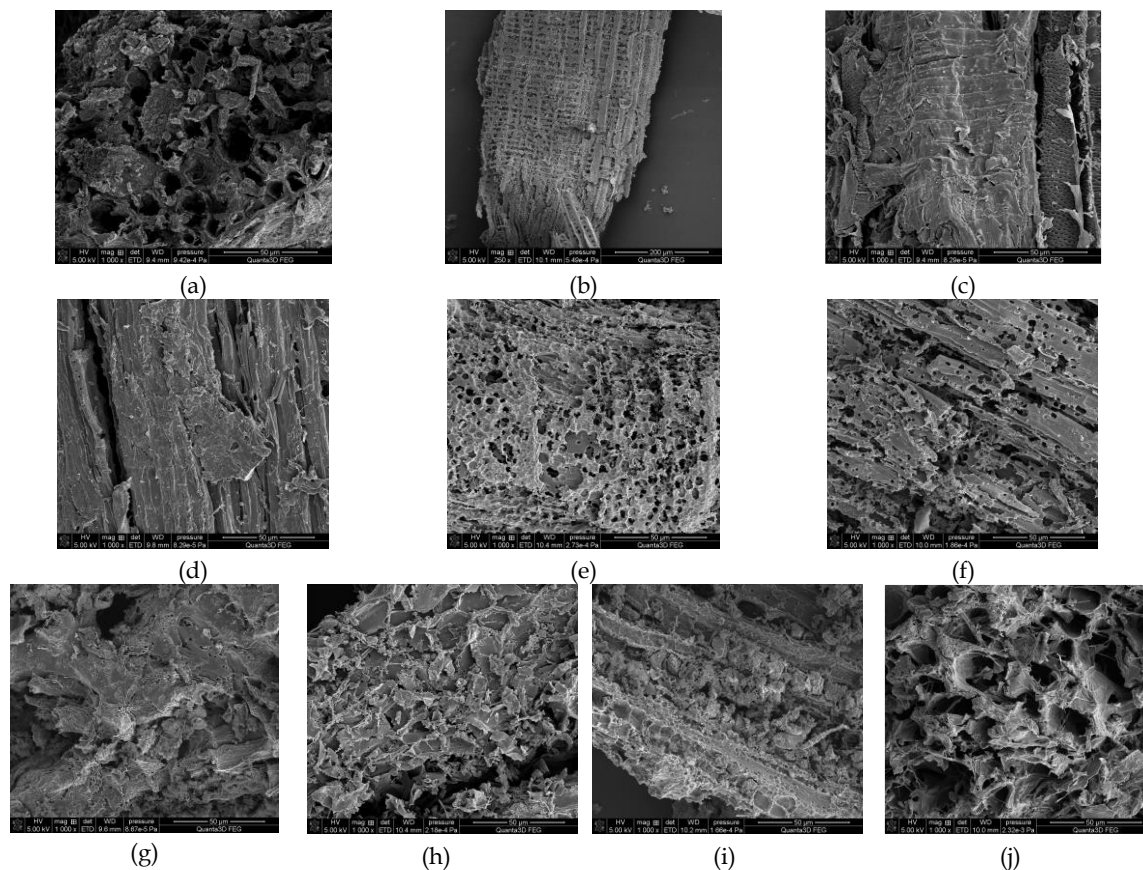
Fig. 2. SEM images for the studied biocarbons: FC (Fir Cone (a), FS (Fir Sawdust) (b), BS (Birch Sawdust (c), HS (Hornbeam Sawdust)) (d), AS (Acacia Sawdust) (e), OS (Oak Sawdust) (f), FB (Fir Bark), (g), AB (Acacia Bark) (h), OB (Oak Bark), (i), BB (Birch Bark) (j)

Table 2 shows the elemental composition of the resulting biocarbons. The content of individual elements in the structure of activated biocarbons is significantly influenced by the type of carbon precursor. The biocarbon obtained from fir cones (FC) is characterized by a relatively large carbon content (82.84%), much smaller hydrogen (0.61%), nitrogen (1.71%), sulfur (0.09%) contents. The biocarbons obtained from sawdust are also characterized by a large content of carbon (89.52%-96.61),

much smaller hydrogen (0.40% - 0.55%), nitrogen (0.09 - 0.54%) contents. The biocarbons obtained from fir bark (FB) and birch (BB) have a slightly smaller carbon content (79.82% and 74.89%, respectively). In turn, the biocarbons obtained from acacia bark (AB) and oak (OB) are characterized by the smallest carbon content (61.40 and 64.39%), respectively. These biocarbons (AB and OB) contain a large amount of ash, which is confirmed by the proximate analysis made based on the TGA data (Table 2). The large carbon content in the obtained materials indicates that the tested carbon precursors (cones, sawdust and bark) are a suitable source of waste material for the biocarbons preparation.

Table 2. The CHNS and proximate analysis results as well as thermostability indices of biocarbons

Biocarbon	C (%)	H (%)	N (%)	S (%)	%H	%A	%VC	%TSC	%C$_{thermo}$
FC	82.84	0.61	1.71	0.09	0.76	0.1	12.2	83.1	87.2
FS	93.24	0.55	0.22	0.24	6.01	4.7	10.0	76.4	88.5
FB	79.82	0.63	1.18	0.12	1.59	7.0	7.9	71.7	90.0
BS	89.52	0.50	0.54	0.48	1.13	6.3	5.6	75.9	93.2
BB	74.89	0.37	1.17	0.15	2.29	15.8	11.0	54.2	83.1
AS	89.88	0.46	0.79	0.27	3.11	8.2	7.4	69.3	90.4
AB	61.40	0.49	1.45	0.23	2.33	36.4	13.8	19.7	58.9
OS	96.61	0.38	0.16	0.31	1.84	8.9	5.2	75.2	93.5
OB	64.39	0.45	1.24	0.20	1.77	33.1	12.7	26.5	67.7
HS	96.04	0.40	0.09	0.22	3.25	4.1	12.2	72.9	85.7

C (%) – the content of carbon; H (%) – the hydrogen content; N (%) – the nitrogen content; S (%) – the sulfur content; %H – moisture; %A – ash; %VC – volatile carbon; %TSC – thermally stable carbon; %C$_{thermo}$ – the thermostable organic matter content, %C$_{thermo}$= %TSC/(%TSC+VC).

The FT-IR (ATR) spectra (Fig. 3 a,b) confirm the presence of aerobic functional groups on the surface of the tested carbons. The low-intensity bands in the range of 3800-3500 cm^{-1} for all analyzed biocarbons correspond to the asymmetric and symmetric tensile vibrations of hydroxyl groups (O-H) (Sen et al., 2011; Vaughn et al., 2013; Marciniak et al., 2018; Ma et al., 2020). The intensity of the bands is stronger for the FB, OB, AB carbons. The bands in the range of 3037-2837 cm^{-1} of small intensity for BS, FB, FS, HS and of slightly larger intensity for BB, OB, OS, AB, AS correspond to the phenolic groups O-H (Figueiredo et al., 1999), which is confirmed by the Boehm method (with the exception for AS and FC, these groups were not identified by the Boehm method (Table 3), while for AS these groups were identified only on the FT-IR (ATR) spectra). In turn, the 2174 cm^{-1} band is associated with the presence of carbon monoxide (CO) in the tested materials (Ma et al. 2020). The bands in the range of 1500 - 1100 cm^{-1} confirm the presence of carbonyl groups (C = O) (bands located at: 1437 cm^{-1} for BB; 1455 cm^{-1} for BS; 1470 cm^{-1} for FB; 1452 cm^{-1} for FS; 1500 cm^{-1} for FC (Fig. 3a) and 1395 cm^{-1} for OS and AS; 1413 cm^{-1} for OB and AB (Fig. 3b)) (Figueiredo et al., 1999), which is also confirmed by the Boehm method (Table 3). In contrast, the bands located at 1560 cm^{-1} for HS, OS and AS are characteristic of the quinone groups (Figueiredo et al., 1999). Moreover, the bands in the range of 1100 - 1000 cm^{-1} are characteristic of the tensile vibrations C-OH (bands located at: 1043 cm^{-1} for BB, BS, FB, FS, FC (Fig. 3a) and 1052 cm^{-1} for HS, AS and AB; 1043 cm^{-1} for OB; 1007 cm^{-1} for OS (Fig. 3b) (Figueiredo et al., 1999). It should be emphasized that various carbon precursors and activation with CO$_2$ change the chemical structure of the surface of the obtained biocarbons.

All analyzed biocarbons have both acidic and basic functional groups on their surface, which is confirmed by the Boehm method (Table 3). However, for almost all biocarbons, alkaline groups prevail on the surface. Most alkaline groups were identified on the surface of biocarbons, where the precursor was the bark. Noteworthy are the two carbons AB and OB, which have almost three times larger content of alkaline groups on the surface. The content of alkaline groups for these carbons is 10 times larger than that of the acidic ones. For all biocarbons from studied acid groups, are mainly carbonyl and carboxyl depending on the carbon precursor (the AS exception does not include the carboxyl groups). It should be noted that only in the case of the AB and OB carbons, the presence of

lactone groups was confirmed. The alkaline nature of biocarbons can be linked to the pyrolysis of biomass, during which carbonates are formed (Ronsse et al., 2012; Spokas et al., 2012; Mukome et al., 2013; Zhao et al., 2017). The content of carbonates (e.g. calcium carbonates) increases with increasing temperature and content of hemicellulose and cellulose in the biomass.

(a)   (b)
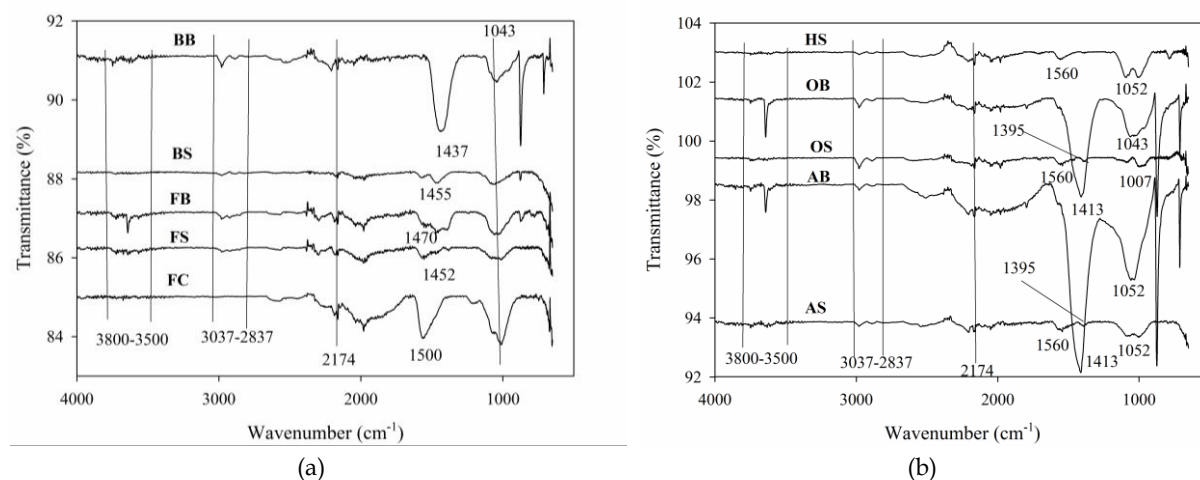
Fig. 3. FT-IR (ATR) spectra for the studied biocarbons (FC (Fir Cone), FS (Fir Sawdust), FB (Fir Bark), BS (Birch Sawdust), BB (Birch Bark), AS (Acacia Sawdust), AB (Acacia Bark), OS (Oak Sawdust), OB (Oak Bark), HS (Hornbeam Sawdust))

Table 3. The biocarbons functional surface groups determined by the Boehm method and the pH_{pzc} values

Biocarbons	Total Basic Groups (mmol/g)	Total Acidic Groups (mmol/g)	Phenolic Groups (mmol/g)	Lactone Groups (mmol/g)	Carboxylic Groups (mmol/g)	Carbonyl Groups (mmol/g)	pH_{pzc}
FC	1.061	0.688	0	0	0	0.688	9.27
FS	0.688	0.623	0	0	0.281	0.342	8.04
FB	1.840	0.375	0	0	0.250	0.125	11.78
BS	0.904	0.406	0	0	0.125	0.281	8.69
BB	0.499	0.421	0	0	0.063	0.374	8.53
AS	1.126	0.625	0	0	0	0.625	9.80
AB	6.474	0.499	0	0.031	0.031	0.437	11.79
OS	2.000	0.405	0	0	0.125	0.296	8.56
OB	5.208	0.593	0	0.094	0.031	0.468	11.98
HS	0.532	0.437	0	0	0.063	0.342	8.39

pH_{pzc} – the point of zero charge

The zero charge point is the pH value at which the surface of the adsorbent in water has a zero electric charge. If the pH of a solid is higher than pH_{pzc}, its surface is negatively charged. However, when the pH is less than pH_{pzc}, then the surface is positively charged. The pH value at which the zero point of a substance (e.g. biocarbon) is located depends on the nature of its surface (Al-Degs et al., 2008; Cardenas-Peña et al., 2012; Lim et al., 2013). The exact pH_{pzc} values derived from the graphs (Fig. 4) are summarized in Table 3. The pH_{pzc} values are consistent with the results obtained by the Boehm's method (Table 3).

Fig. 5a-f presents the results of thermal analysis of the tested biocarbons. The differences in the course of the analyzed curves obtained for the materials from bark (Fig. 5a-c) and sawdust (Fig. 5 d-f) are clearly visible. The degradation of biocarbons obtained from the bark proceeds in 2 stages. The first stage takes place in the temperature range of 300-550 °C. The second stage occurs in the range of 700 - 800 °C. In all cases, the mass loss in the first stage is greater than in the second stage (Fig. 5a) which indicates a greater share of small structures in these carbons. The two-step degradation course

is clearly visible on the DTG (Fig. 5b) and DTA (Fig. 5c) curves. The visible peaks are wide, indicating a large range of temperatures of the mass loss (Fig. 5b) and the exothermic decomposition of biocarbons (Fig. 5c). It is important that the materials obtained from the bark, especially carbons from acacia (AB) and oak (OB) barks have a large ash content of 36.4% and 33.1%, respectively.
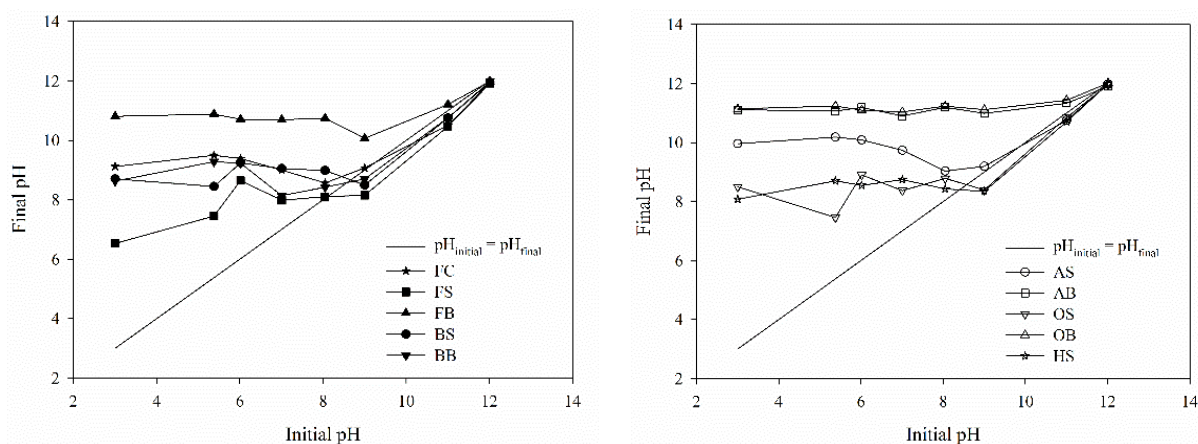

Fig. 4. pH_{pzc} for the studied biocarbons (FC (Fir Cone), FS (Fir Sawdust), FB (Fir Bark), BS (Birch Sawdust), BB (Birch Bark), AS (Acacia Sawdust), AB (Acacia Bark), OS (Oak Sawdust), OB (Oak Bark), HS (Hornbeam Sawdust))

The course of the thermal degradation of the biocarbons obtained from sawdust was slightly different (Fig. 5 d-f). The materials decomposition began at 300 – 400 °C and proceeded in one stage. The most stable are the carbons obtained from the sawdust of oak (OS) and hornbeam (HS). The biocarbon obtained from fir, both sawdust (FS, Fig. 5d) and bark (FB, Fig. 5a), decomposed the fastest. This is due to the different structures of the coniferous wood compared to the deciduous wood. The coniferous wood has a smaller density, is softer and less resistant to heat treatment than the hardwood from the deciduous trees. These characteristics affect the course of the pyrolysis and activation processes as well as the parameters of the resulting product. The diverse course of the analyzed curves indicates that the properties of the obtained active biocarbons are significantly affected by the structure and composition of the initial precursor, which was mentioned when discussing the SEM images. The biocarbons obtained from three different precursors from the fir tree cones, bark and sawdust are additionally compared in Fig. 5g-i. In conclusion, the carbon obtained from the cones is the most thermally stable.

On the basis of thermal analysis conducted in the O_2 and N_2 atmospheres, an approximate assessment of the type of carbonaceous matter in the studied biocarbons was made. The results of moisture (%H), ash (%A), volatile carbon (%VC) and thermally stable carbon (%TSC) in the biocarbons are summarized in Table 2. The tested biocarbons were characterized by the small moisture content. The ash content varied, but it is clear that the biocarbons obtained from the bark have a greater share of minerals. In the case of the biocarbon from the acacia bark it was as much as 36.4%. The materials with a large ash content have also a larger %VC content and a smaller %TSC content compared to the biocarbons obtained from the sawdust of some types of trees. This may be due to the differences in the structure of wood waste, contamination of the bark of starting materials or too intense activation. The proportion of the stable fraction (%C_{thermo}) indicates a large content of the stable carbon fraction. A different relationship can be observed for the materials obtained from the cones, sawdust and fir bark. In this case, the biocarbon obtained from the sawdust was characterized by a larger content of both volatile compounds (%VC) and thermally resistant (%TSC). This may be due to different compositions of the starting materials compared to the deciduous trees, which contain larger amounts of resin oils.

When comparing the adsorption properties of the obtained biocarbons (Table 4), the selection of the carbon precursor plays an important role. For all tested biocarbons, comparing two carbon precursors, i.e. sawdust and bark, the biocarbons obtained from the bark are better adsorbents. Comparing the three carbon precursors of the cone, bark, sawdust, the best adsorbent proved to be the
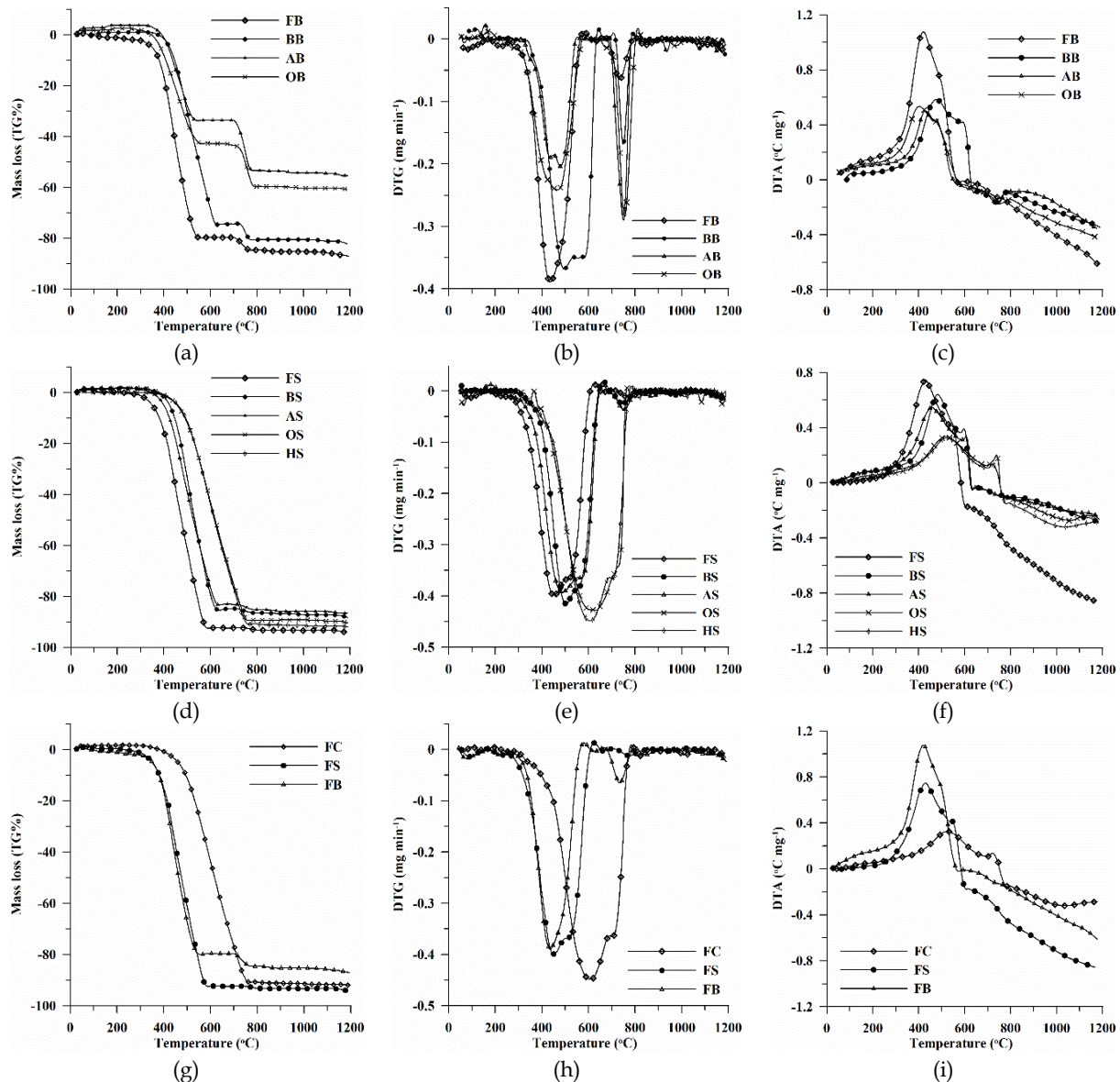
Fig. 5. TG% (a,d,g), DTG (b,e,h) and DTA (c,f,i) curves for the studied biocarbons (FC (Fir Cone), FS (Fir Sawdust), FB (Fir Bark), BS (Birch Sawdust), BB (Birch Bark), AS (Acacia Sawdust), AB (Acacia Bark), OS (Oak Sawdust), OB (Oak Bark), HS (Hornbeam Sawdust))

biocarbon obtained from the cones, slightly poorer from the bark. It should be noted that the porous structure has a significant impact on the adsorption properties of the obtained biocarbons. The dependence of the effect of the porous structure parameters on the adsorption properties of the studied biocarbons was observed, the larger the specific surface area and thus the more developed the porous structure of the tested adsorbents, the better the adsorption properties of the biocarbons in relation to ammonia. For example, the biocarbon FC has the largest adsorption capacity of ammonia (2.93 mmol/g; 20 °C). This material has the largest specific surface area of the analyzed biocarbons (1286 m²/g). The presence of the surface functional groups on the surface of the biocarbons under study can play an important role. Analyzing the ammonia TPD data for the studied biocarbons, it was found that the tested carbon materials adsorbed a relatively large amount of ammonia, while a small part of it was desorbed. Taking this into account, it can be concluded that the analyzed biocarbons are promising materials for capturing the environmentally harmful gas ammonia.

The obtained experimental data (Table 4) were compared with the data available in the literature for other carbon adsorbents (Table 5). It was shown that the tested biocarbons are characterized by good adsorption properties.

Table 4. The NH_3 adsorption capacity and TPD for the tested biocarbons

Biocarbons	NH_3 Adsorption Capacity (mmol/g) p ~ 750 mmHg		NH_3 TPD (mmol/g) p ~ 750 mmHg	
T (°C)	0	20	0–250	20–250
FC	0.96	2.93	0.27	0.40
FS	0.75	1.86	0.17	0.26
FB	2.40	0.91	0.24	0.19
BS	1.70	0.82	0.27	0.19
BB	2.59	0.65	0.22	0.16
AS	1.82	0.78	0.42	0.22
AB	2.15	0.95	0.23	0.18
OS	1.55	0.80	0.16	0.12
OB	0.87	2.10	0.24	0.20
HS	1.99	0.92	0.20	0.14

Table 5. Comparison of the maximum adsorption capacity gas ammonia of the prepared activated biocarbons with that of other carbon materials

Carbon materials	S_{BET} m²/g	Adsorption capacity (mmol/g)	References
FC	1286	0.96 – 2.93	This study
FS	898	0.75 – 1.86	This study
FB	746	0.91 – 2.40	This study
BS	866	0.82 – 1.70	This study
BB	553	0.65 – 2.59	This study
AS	783	0.78 – 1.82	This study
AB	555	0.95 – 2.15	This study
OS	609	0.80 – 1.55	This study
OB	515	0.87 – 2.10	This study
HS	695	0.92 – 1.99	This study
OAK-250-KOH [1]	-	1.47	(Takaya et al., 2015)
OAK-450-KOH [2]	-	0.35	(Takaya et al., 2015)
OAK-250-H_2O_2 [3]	-	1.47	(Takaya et al., 2015)
OAK-450-H_2O_2 [4]	-	0.59	(Takaya et al., 2015)
AA-WS250-AR [5]	851	3.11	(Ro et al., 2015)
AC [6]	430	0.78 - 4.19	(Helminen et al., 2001)
AC [7]	450	0.77 - 5.08	(Helminen et al., 2001)
Na-OH-AC [8]	1125	1.69	(Liu and Aika, 2003)
HNO_3-AC [9]	1010	3.07	(Liu and Aika, 2003)
H_2SO_4-AC [10]	1016	2.78	(Liu and Aika, 2003)
AC [11]	1161	1.19	(Liu and Aika, 2003)
BC-1-CO_2-6h* [12]	884	1.06 - 2.69	(Jedynak and Charmas, 2021)
BC-1-CO_2-12h* [13]	1049	0.82 - 3.59	(Jedynak and Charmas, 2021)
BC-1-CO_2-6h [14]	1181	1.13 - 5.18	(Jedynak and Charmas, 2021)
BC-2-CO_2-6h [15]	1167	0.95 - 3.95	(Jedynak and Charmas, 2021)

[1,2] hydrochar from the oak wood, pyrolysis at 250°C or 450°C, activation with KOH; [3,4] hydrochar from the oak wood, pyrolysis at 250°C or 450°C, activation with H_2O_2; [5] biochars from the wood shaving waste, pyrolysis at 250°C, activation with H_3PO_4; [6] activated carbon (Aldrich Darco); [7] activated carbon (Merk); [8] active carbon pyrolysis at 773 K, activated by impregnation $NaNO_3$ in water; [9,10] active carbons, pyrolysis at 773 K, activated by the aqueous HNO_3 or H_2SO_4 solution; [11] active carbon pellets; [12-15] biochar from the spruce cones, pyrolysis at 800°C or 850°C, activated by CO_2.

4. Conclusions

It was proved that various carbon precursors (wood waste) can be successfully used as an economical precursor for the production of effective carbon adsorbents with very good porous structure parameters: large specific surface area, large pore volume, and as a result good adsorption capacity. It should be emphasized that the porous structure has a significant impact on the adsorption properties of the obtained biocarbons. The higher the value of the specific surface area, the better the adsorption properties towards ammonia were shown by the tested adsorbents. The physicochemical and adsorption properties are significantly affected by the structure and composition of the initial precursors: wood species, waste structure (bark, sawdust, cone), and hardness. All tested activated biocarbons are characterized by significant thermal stability and are effective adsorbents for ammonia removal from the gas phase. Moreover, its very small amount is desorbed, so the resulting biocarbons can be promising as far as the capture of NH_3 and possibly other toxic gases is concerned. Therefore, the important aspect of research is the use of modern technologies and methodologies for the production of biocarbon materials with controlled properties. The application of advanced chemical techniques, using a variety of waste materials, can lead to obtaining better developed and efficient biocarbons. This is a desirable trend in the conscious protection of the natural environment.

Acknowledgments

References

AL-DEGS, Y.S., EL-BARGHOUTHI, M.I., EL-SHEIKH, A.H., WALKER, G.M., 2008. *Effect of solution pH, ionic strength, and temperature on adsorption behavior of reactive dyes on activated carbon*. Dyes Pigm. 77, 16–23.

BALT, M., 2011. *Production of bioethanol from lignocellulosic materials via the biochemical pathway. A review.* Energ. Conver. Manage, 52, 858-875.

BASHARNAVAZ, H., HABIBI-YANGJEH, A., PIRHASHEMI, M., 2020. *Graphitic carbon nitride as a fascinating adsorbent for toxic gases: A mini-review*, Chem. Phys. Lett. 754, 137676.

BAZAN-WOŹNIAK, A., NOWICKI, P., PIETRZAK, R., 2017. *The influence of activation procedure on the physicochemical and sorption properties of activated carbons prepared from pistachio nutshells for removal of NO₂/H₂S gases and dyes.* J. Clean. Prod. 152, 211-222.

BOEHM, H.P., 2002. *Surface oxides on carbon and their analysis: A critical assessment*. Carbon 40, 145–149.

BOGUMIŁ, D. *Wpływ metod obróbki wstępnej biomasy na wydajność otrzymywania biogazu*. 2016. Stud. Ecolog. Bioethic. 14, 191-203.

BORHAN, A., TAHA, M.F., HAMZAH, A.A., 2014. *Characterization of activated carbon from wood sawdust prepared via chemical activation using potassium hydroxid*e. Adv. Mater. Res. 832, 132-137.

BRUNAUER, S., EMMETT, P.H., TELLER, E., 1938. *Adsorption of gases in multimolecular layers*. J. Am. Chem. Soc. 60, 309-319.

BŘENDOVÁ, K., SZÁKOVÁ, J., LHOTKA, M., KRULIKOVSKÁ, T., PUNČOCHÁŘ, M., TLUSTOŠ, P., 2017. *Biochar physicochemical parameters as a result of feedstock material and pyrolysis temperature: Predictable for the fate of biochar in soil?* Environ. Geochem. Health 39, 1381-1395.

CALVELO PEREIRA, R., KAAL, J., CAMPS ARBESTAIN, M., PARDO LORENZO, R., AITKENHEAD, W., HEDLEY, M., MSCÍAS, F., HINDMARSH, J., MACIÁ-AGULLÓ, J.A., 2011. *Contribution to characterisation of biochar to estimate the labile fraction of carbon*. Org. Geochem. 42, 1331–1342.

CÁRDENAS-AGUIAR, E., GASCÓ, G., PAZ-FERREIRO, J., MÉNDEZ, A., 2019. *Thermogravimetric analysis and carbon stability of chars produced from slow pyrolysis and hydrothermal carbonization of manure waste*. J. Anal. Appl. Pyrol. 140 434–443.

CHEN, Y., LI, L., LI, J., OUYANG, K., YANG, J., *Ammonia capture and flexible transformation of M-2(INA) (M=Cu, Co, Ni, Cd) series materials*. J. Hazard. Mater. 306, 340–347 (2016).

CHO, D.W., KIM, S. TSANG, Y.F., SONG, H., 2019. *Preparation of nitrogen-doped Cu-biochar and its application into catalytic reduction of p-nitrophenol*. Environ. Geochem. Health 41, 1729-1737.

CONTESCU C.I., ADHIKARI, S.P., GALLEGO, N.C., EVANS, N.D., BISS, B.E., 2018. *Activated carbons derived from high-temperature pyrolysis of lignocellulosic biomass*. J. Carbon Res. 4, 51HUANG, C.C., LI, H.S., CHEN, C.H., 2008. *Effect of surface acidic oxides of activated carbon on adsorption of ammonia*. J. Hazard. Mater. 159, 523–527.

FIGUEIREDO, J.L., PEREIRA, M.F.R., FREITAS, M.M.A., ÓRFAO, J.J.M., 1999, *Modification of the surface chemistry of activated carbons*. Carbon 37, 1379–1389.

HELMINEN, J., HELENIUS, J., PAATERO, E., TURUNEN, I., 2001. *Adsorption equilibria of ammonia gas on inorganic and organic sorbents at 298.15 K*. J. Chem. Eng. Data 46, 391–399.

JAGIELLO, J., OLIVIER, J.P., 2013. *2D-NLDFT Adsorption models for carbon slit-shaped pores with surface energetical heterogeneity and geometrical corrugation*. Carbon 55, 70–80.

JAGIELLO, J., OLIVIER, J.P., 2013a. *Carbon slit pore model incorporating surface energetical heterogeneity and geometrical corrugation*. Adsorption 19, 777–783.

JEDYNAK, K., CHARMAS, B., 2021. *Preparation and Characterization of physicochemical properties of spruce cone biochars activated by CO_2*. Materials 14, 3859.

KRUK, M., JARONIEC, M., 2001. *Gas adsorption characterization of ordered organic-inorganic nanocomposite materials*. Chem. Mater. 13, 3169–3183.

LALAK, J. KASPRZYCKA, A., MURAT, A., PAPROTA, E.M. TYS, J., 2014. *Obróbka wstępna biomasy bogatej w lignocelulozę w celu zwiększenia wydajności fermentacji metanowej*. Acta Agrophys. 21, 51-62.

LIM, C.K., BAY, H.H., NOEH, C.H., ARIS, A., MAJID, Z.A., IBRAHIM, Z., 2013. *Application of zeolite-activated carbon macrocomposite for the adsorption of Acid Orange 7: isotherm. kinetic and thermodynamic studies*. Environ. Sci. Pollut. Res. 20, 7243–7255.

LIU, C. Y., AIKA, K., 2003. Effect of surface oxidation of active carbon on ammonia adsorption. Bull. Chem. Soc. Jpn. 76, 1463–1468.

MA, R., MA, Y., GAO, Y., CAO, J., 2020. *Preparation of micro mesoporous carbon from seawater impregnated sawdust by low temperature one step CO_2 activation for adsorption of oxytetracycline*. SN Appl. Sci. 2, 171-185.

MARCINIAK, M., GOSCIANSKA, J., PIETRZAK, R., 2018. *Physicochemical characterization of ordered mesoporous carbons functionalized by wet oxidation*. J. Mater. Sci., 53, 5997–6007.

MUKOME, F.N.D., ZHANG, X., LUCAS, C.R.S., SIX, J., PARIKH, S.J., 2013. *Use of chemical and physical characteristics to investigate trends in biochar feedstocks*. J. Agric. Food. Chem. 61, 2196–2204.

NOR, N.M.; LAU, L.C., LEE, K.T., MOHAMED, A.R., 2013. *Synthesis of activated carbon from lignocellulosic biomass and its applications in air pollution control – A review*. J. Environ. Chem. Eng. 1, 658–666.

NOWICKI, P., KRUSZYŃSKA, I. PRZEPIÓRSKI, J., PIETRZAK, R., 2013. *The effect of chemical activation method on properties of activated carbons obtained from pine cones*. Cent. Eur. J. Chem., 11, 78–85.

NOWICKI, P., GRUSZCZYŃSKA, K., URBAN, T., WIŚNIEWSKA, M., 2022. *Activated biochars obtained from post-fermentation residue as potential adsorbents of organic pollutants from the liquid phase*. Physicochem. Probl. Miner. Process 58, 146357.

CARDENAS-PEÑA, A.M., IBANEZ, J.G., VASQUEZ-MEDRANO, R., 2012. *Determination of the point of zero charge for electrocoagulation precipitates from an iron anode*, Int. J. Electrochem. Sci. 7, 6142-6153.

RIVERA-UTRILLA, J., BAUTISTA-TOLEDO, I., FERRO-GARCÍA, M.A., MORENO-CASTILLA, C., 2001. *Activated carbon surface modifications by ad-sorption of bacteria and their effect on aqueous lead adsorption*. J. Chem. Technol. Biotechnol. 76, 1209–1215.

RO, K.S., LIMA, I.M., REDDY, G.B., JACKSON, M.A., GAO, B., 2015. *Removing gaseous NH_3 using biochar as an adsorbent*. Agriculture 5, 991–1002.

ROBAK, K., BALCEREK, M., 2017. *Rola obróbki wstępnej biomasy lignocelulozowej w produkcji bioetanolu II generacji*. Acta Agroph. 24, 301-318.

RODRIGUES, C.C., MORAES JR., D., NÓBREGA, S.W., BARBOZA, M.G., 2007. *Ammonia adsorption in a fixed bed of activated carbon*. Biores. Technol. 98, 886–891.

RONSSE, F., VAN HECKE, S., DICKINSON, D., PRINS, W., 2012. *Production and characterization of slow pyrolysis biochar: influence of feedstock type and pyrolysis conditions*. Glob. Chang. Biol. Bioenergy 5, 104–115.

SAAD, M., BIAŁAS, A., GRZYWACZ, P., CZOSNEK, C., SAMOJEDEN, B., MOTAK, M., 2020. *Selective catalytic reduction of NO with ammonia at low temperature over Cu-promoted and N-modified activated carbon*. Chem. Process Eng. 41, 59–67.

SALETNIK, B.; ZAGUŁA, G.; GRABEK-LEJKOo, D.; KASPRZYK, I.; BAJCAR, M.; CZERNICKA, M.; PUCHALSKI, C., 2017. *Biosorption of cadmium(II), lead(II) and cobalt(II) from aqueous solution by biochar from cones of larch (Larix decidua Mill. subsp. decidua) and spruce (Picea abies L. H. Karst)*. Environ. Earth Sci. 76, 574–584.

SAMOJEDEN, B., GRZYBEK, T., 2016. The influence of the promotion of N-modified activated carbon with iron on NO removal by NH_3-SCR (Selective catalytic reduction). Energy 116, 1484-1491.

SAMOJEDEN, B., GRZYBEK, T., 2017. *The influence of nitrogen groups introduced onto activated carbons by high or low-temperature NH_3 treatment on SO_2 sorption capacity.* Ads. Sci. Technol. 35, 572–581.

SAYAGO, I., SANTOS, H., HORRILLO, M.C., ALEIXANDRE, M., FERNÁNDEZ, M.J., TERRADO, E., TACCHINI, I., AROZ, R., MASER, W.K., BENITO, A.M., MARTÍNEZ, M.T., GUTIÉRREZ, J. MUÑOZ, E., 2008. *Carbon nanotube networks as gas sensors for NO_2 detection*. Talanta 77, 758-764.

SEN, T.K., AFROZE, S., ANG, H.M., 2011. *Equilibrium, kinetics and mechanism of removal of methylene blue from aqueous solution by adsorption onto pine cone biomass of Pinus radiate.* Water Air Soil Pollut. 218, 499–515.

SPOKAS, K.A., CANTRELL, K.B., NOVAK, J.M., ARCHER, D.W., IPPOLITO, J.A., COLLINS, H.P., BOATENG, A.A., LIMA, I.M., LAMB, M.C., MCALOON, A.J., LENTZ, R.D., NICHOLS, K.A., 2012. *Biochar: a synthesis of its agronomic impact beyond carbon sequestration*. J. Environ. Qual. 41, 973–989.

TAKAYA, C.A.; PARMAR, K.R.; FLETCHER L.A.; ROSS, A.B., 2019. *Biomass-derived carbonaceous adsorbents for trapping ammonia.* Agricultur*e* 9, 16–30.

VAUGHN, S.F., KENAR, J.A., THOMPSON, A.R., PETERSON, S.C., 2013. *Comparison of biochars derived from wood pellets and pelletized wheat straw as replacements for peat in potting substrates*. Ind. Crops. Prod. 51, 437-443.

WIŚNIEWSKA, M., MARCINIAK, M., GĘCA, M., HERDA, K., PIETRZAK, R., NOWICKI, P., 2022. Activated biocarbons obtained from plant biomass as adsorbents of heavy metal ions, Materials, 15, 5856.

YANG, H., WANG, Y., LIU, Z., LIANG, D., LIU, F., ZHANG, W., DI, X., WANG, C., HO, S.-H., CHEN, W.-H., 2017. *Enhanced thermal conductivity of waste sawdust-based composite phase change materials with expanded graphite for thermal energy storage*. Bioresour. Bioprocess. 4 , 1–12.

YEOM, C., KIM, Y., 2017. *Adsorption of ammonia using mesoporous alumina prepared by a templating method*. Environ. Eng. Res. 22, 401–406.

ZIĘZO, M., CHARMAS, B., JEDYNAK, K., HAWRYLUK, M., KUCIO, K., 2020. *Preparation and characterization of activated carbons obtained from the waste materials impregnated with phosphoric acid(V).* Appl. Nanosci. 10/12, 4703-4716.

ZHAO, S-X., NA, T., WANG, X-D., 2017. *Effect of temperature on the structural and physicochemical properties of biochar with apple tree branches as feedstock material*. Energies 10, 1293.